

Electromagnetic Background Rate Studies (for different solenoid magnet fields and FDC hole sizes)

A. Somov, *JLAB*

Abstract

We studied the impact of the solenoid magnet field on the electromagnetic background rate in the GlueX sub-detectors. The rate in the FDC chambers has also been studied for various sizes of insensitive region around the beamline.

1 Introduction

The electromagnetic background rates were studied for three solenoid magnet field maps corresponding to the default value of the B-field, and 80% and 70% of the default B-field. The field maps were produced by David Lawrence using a Poisson Superfish program. The rate in the Start Counter and FDC were also compared with that obtained using the old solenoid magnet field map created using TOSCA magnetic field simulation program. The simulation is based on the reconstruction lib release 2010-02-11. In the simulation, we set a threshold of 1.2 MeV on the low energy of the beam photons. The electromagnetic background rates were normalized assuming operation of the GlueX detector at high-luminosity of 10^8 photons per seconds.

We observed a relatively large rate in the FDC pad chambers of the most upstream package in strips situated close to the beamline. We studied the impact of the chamber's insensitive region around the beamline on the electromagnetic background rate and acceptance of some typical exotic meson decays.

2 Electromagnetic Background Rate

2.1 Start Counter

We used the latest geometry (svn revision r3083) of the Start Counter provided by W.Boeglin. The SC consisted of 40 scintillator paddles, each of which is about 600 mm

long, 10 cm wide, and 3 mm thick. The size of the hole in the downstream end of the SC corresponds to 2 cm. The energy deposited by Geant in the SC paddle by particles produced in the electromagnetic interactions is shown in Fig. 1. The energy is computed at the end of the light guide assuming a light attenuation length of 150 cm. In the analysis we applied an energy threshold of 0.1 MeV.

The SC paddle rate induced by the electromagnetic background for the default, 80%, and 70% values of the solenoid magnet field is presented in Fig. 2. As follows from this plot, decreasing the magnetic field to the 70% of the nominal B-field value, increases the paddle rate from 100 kHz/paddle to about 160 kHz/paddle. The probability of having a random coincidence hit from the electromagnetic background in a 2-paddle wide cluster is estimated to be relatively small; in the 50 ns time interval it can be estimated as $w = 160 \cdot 10^3 \cdot 50 \cdot 10^{-8} \cdot 2 = 1.8 \cdot 10^{-2}$. However, the Geant simulation might underestimate the electromagnetic background rate, so that the double-hit probability might become critical for operating the SC at high luminosity.

Comparison of the SC rate for two field maps obtained using the ANSYS and Poisson Superfish programs is presented in Fig 3. The Poisson Superfish field map predicts about 20% smaller rate in the SC.

2.2 CDC

The electromagnetic background rate per CDC wire for different CDC layers is presented in Fig. 4. As expected, the CDC is not very much sensitive to the magnetic field variations. The electromagnetic background rate increases by about 15% in the CDC layers positioned close to the beamline when the magnetic field is reduced to 70% of the nominal B-field value. The maximum rate is found in the 1st CDC layer and constitute about 30 kHz/wire.

2.3 FCAL

The electromagnetic background rate in the FCAL is presented in Fig. 5. The cell energy threshold corresponded to the default value of 20 MeV¹. As can be seen from the right plot of Fig. 5, the B-field variations in our range almost does not affect the FCAL rate. The maximum rate in the FCAL block closest to the beamline was found to be about 2.4 MHz.

2.4 TOF

The TOF hits were taken from the DTOFMCRresponse factory. The simulated PMT response in the ADC channels², produced by a minimum ionizing pion originating from the target region and penetrating the paddle close to the PMT and at the opposite side

¹The hits were taken from the DFCALHit table. The Geant energy released in the block was attenuated to the end of the block and smeared according to photon-statistics resolution

²TOF calibration will be refined in the future.

of the paddle is shown in the left plot of Fig. 6. The arrow on this plot denotes the ADC threshold used for the rate estimates. The ADC distribution originating from the electromagnetic background is presented in the right plot of Fig. 6. The TOF rate per paddle (per readout channel) is shown in Fig. 7. The left plot represents the rate in the upstream (layer 0) and downstream (layer 1) layers. The occupancy in the upstream TOF layer is found to be about a factor of 1.6 larger than that in the downstream layer³. The maximum rate of about 12 MHz per PMT was found in the long paddle situated closest to the beamline, paddles number 20 and 21. In order to reduce the rate in these paddles we might consider to split each of this paddles into two. The TOF rate for different values of the magnetic field is shown in the right plot of Fig. 7. The rate increases by about 15% when the field is lowered to 70% of the default value. The maximum TOF rate in the paddles #20 and #21 as a function of the ADC threshold is presented in Fig. 8.

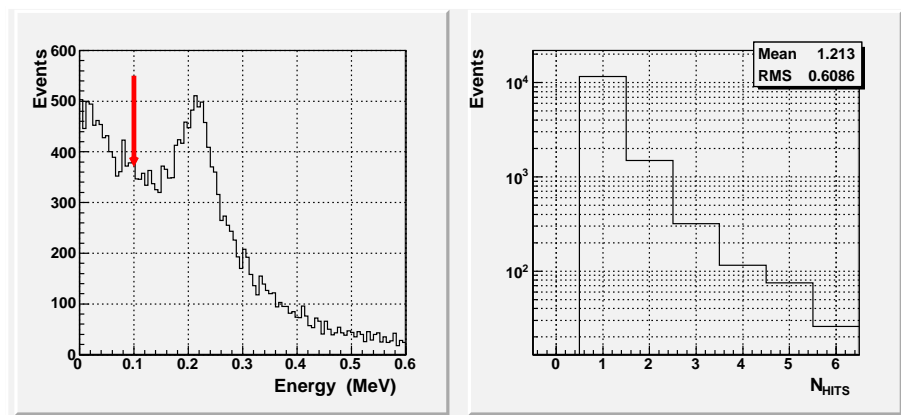


Figure 1: Energy deposited in the paddles of the start counter by particles produced in electromagnetic interactions (left). Arrow indicates the energy threshold of 0.1 MeV applied in the analysis. Start Counter hit multiplicity for electromagnetic background events is presented in the right plot.

3 FDC

The FDC analysis was organized into several steps:

- First, we considered the rate of the wire and pad chambers for the default geometry.
- We studied the impact of the cathode material around the beamline on the rate in pad chambers.
- We studied the rate dependence from the sizes of the chamber's insensitive areas around the beamline.

³The rate in the upstream layer was about 1.3 time larger when RICH material was presented in the simulation

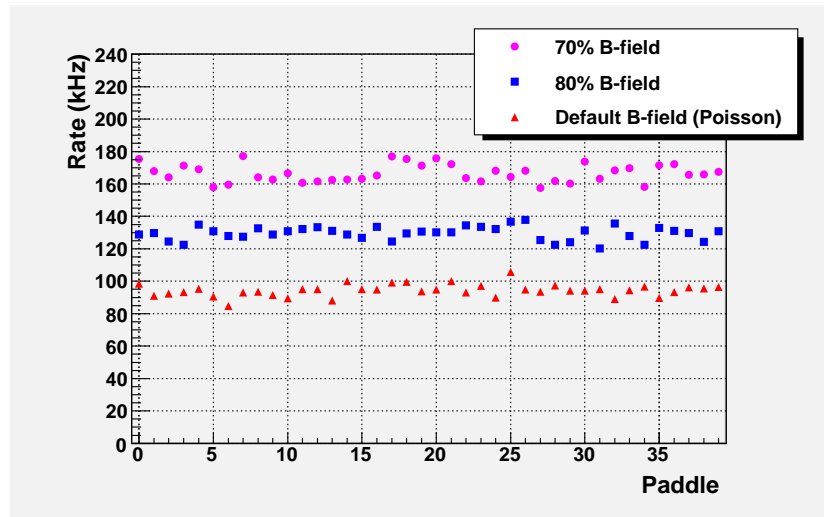


Figure 2: Start Counter paddle rate induced by the electromagnetic background. Polymarkers correspond to the three different values of the B-field: default (triangles), 80% B-field (boxes), and 70% B-field (circles). The magnetic field maps were obtained using the Poisson Superfish program.

- We estimated the effect of the magnetic field on the rate.

4 Summary

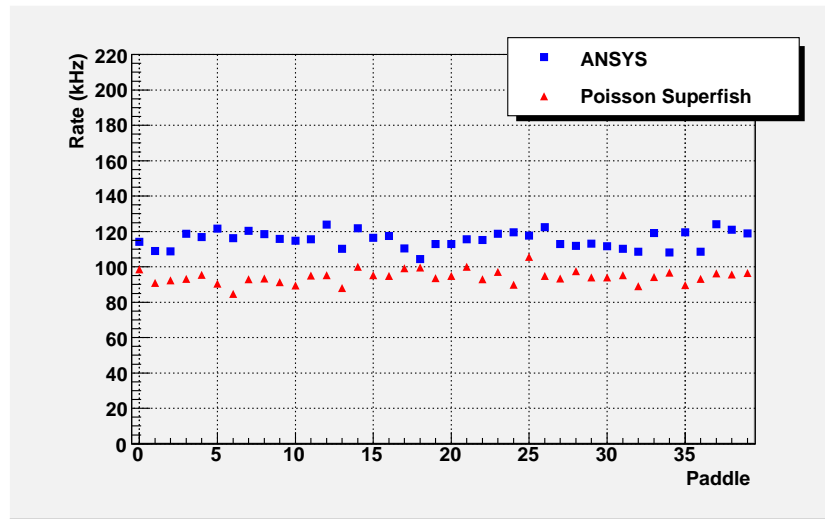


Figure 3: Start Counter paddle rate obtained using the solenoid magnet field map produced by ANSYS (boxes) and Poisson Superfish (triangles) program. The maps were generated according to the default value of the B-field.

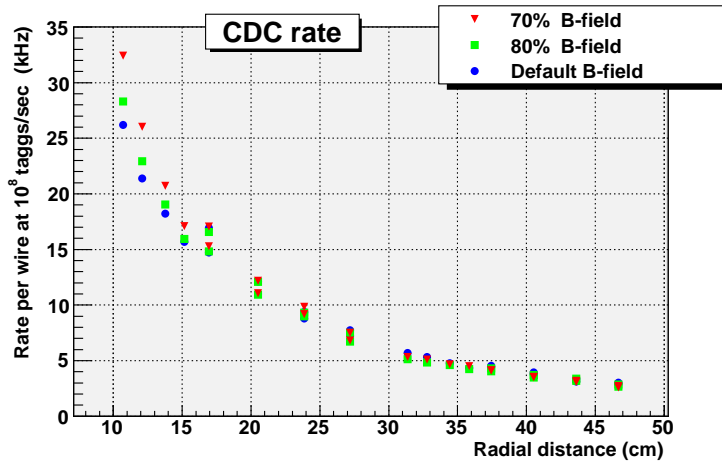


Figure 4: CDC rate per wire induced by the electromagnetic background for the CDC layers positioned at different radial distances from the beamline. Circles, boxed, and triangles correspond to the default, 80% B-field, and 70% B-field, respectively.

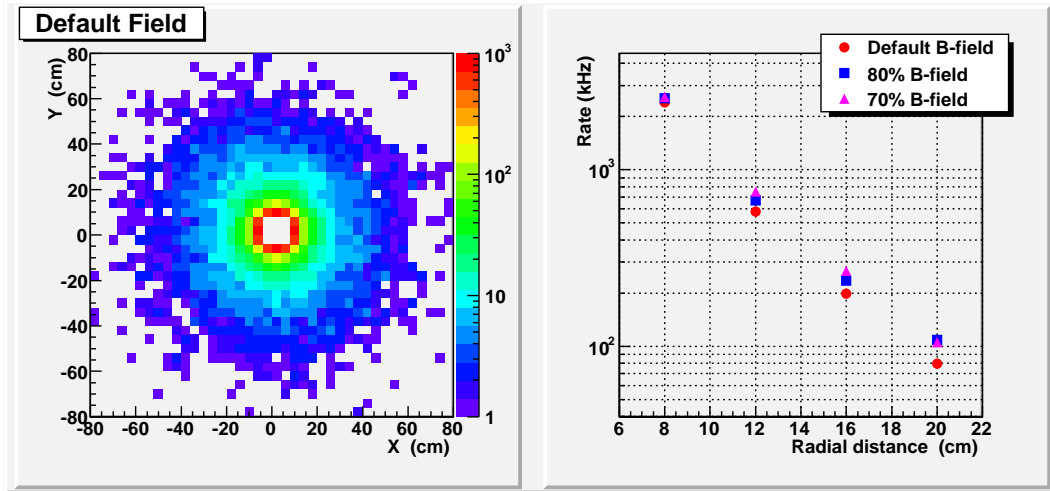


Figure 5: FCAL rate per readout channel induced by the electromagnetic background. On the right plot, the rate is plotted for three B-field values as a function of the radial distance of the glass block from the beamline.

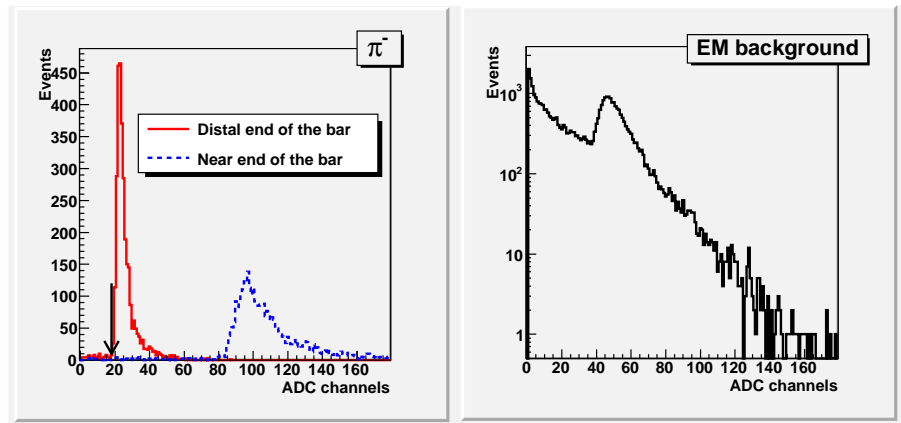


Figure 6: Simulated PMT responses in ADC channels produced by relativistic tracks penetrating the TOF paddle at the near (blue) and distal (red) ends (left plot). The arrow indicates the ADC threshold used in the analysis. ADC response induced by the electromagnetic background (right).

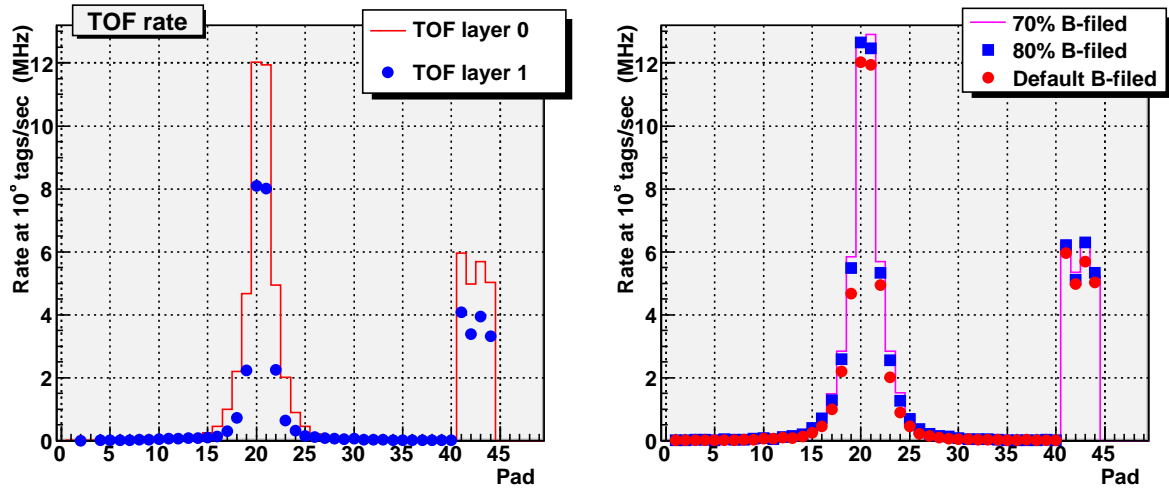


Figure 7: TOF rate per readout channel as a function of the paddle number. The rate in the upstream (solid curve) and downstream (circles) TOF layers is presented in the left plot. The TOF rate in the upstream layer for different values of the magnetic field is shown in the right plot. The paddles 20 and 21 are the long paddles positioned adjacent to the beamline.

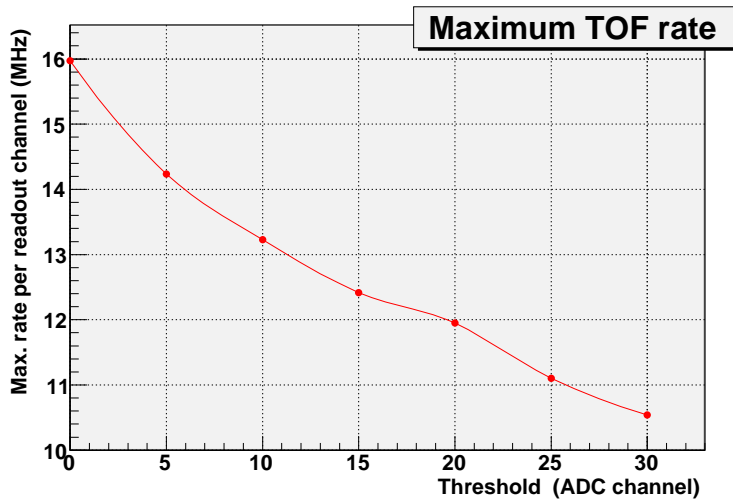


Figure 8: Maximum rate per PMT (in the long TOF paddles #20 and #21 positioned near the beamline) induced by the electromagnetic background as a function of the ADC threshold.

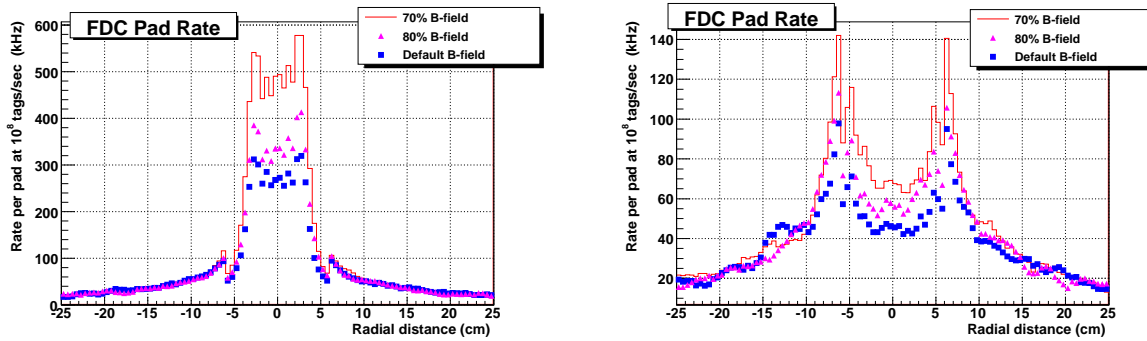


Figure 9: FDC rate per paddle induced by the electromagnetic background for the most upstream pad chambers (left) and most downstream pad chambers (right). Circles, boxed, and triangles correspond to the default, 80%, and 70% B-field, respectively.

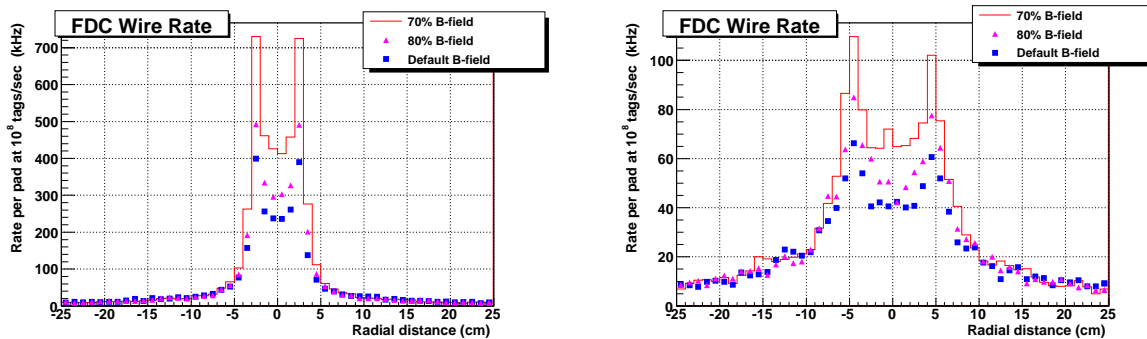


Figure 10: FDC rate in wire chambers per wire induced by the electromagnetic background for the most upstream wire chambers (left) and most downstream wire chambers (right). Circles, boxed, and triangles correspond to the default, 80%, and 70% B-field, respectively.

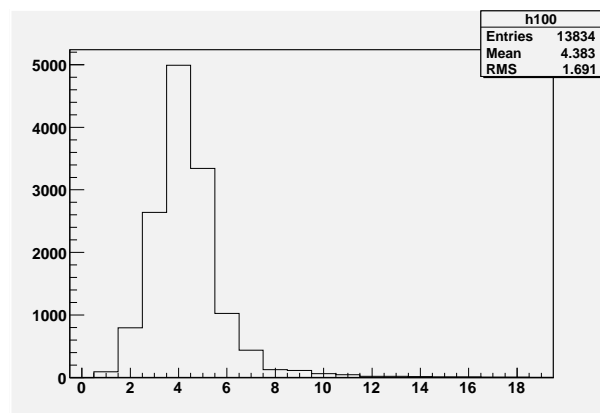


Figure 11: FDC pad multiplicity in the electromagnetic background.

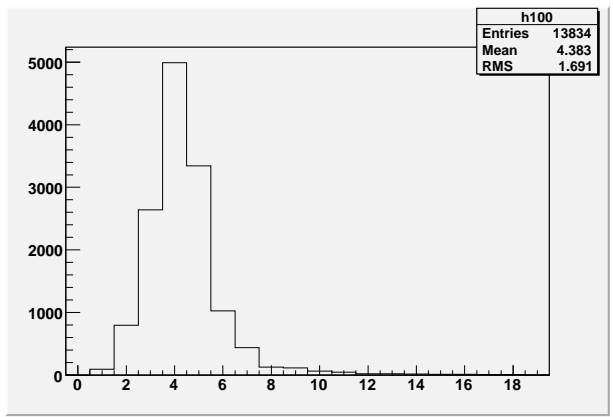


Figure 12: FDC rate per strip averaged over 24 strips located around the beamline for different radii, R , of the the copper cathodes: default geometry (circles), $R = 1.3$ cm (boxes), $R = 1.7$ cm (triangles), and $R = 2.1$ cm (open circles).